Simulation of magnetic control of the plasma shape on the DEMO tokamak

M. Ariola[a,b,*], A. Pironti[c,b], R. Ambrosino[c,b], M. Mattei[d,b], W. Biel[e], T. Franke[f,g]

[a]*Dipartimento di Ingegneria, Università degli Studi di Napoli Parthenope, 80143 Napoli, Italy*
[b]*Consorzio CREATE, via Claudio 21, 80125 Napoli, Italy*
[c]*DIETI, Università degli Studi di Napoli Federico II, 80125 Napoli, Italy*
[d]*Dipartimento di Ingegneria, Università degli Studi della Campania "Luigi Vanvitelli", 80131 Aversa, Italy*
[e]*Institute of Energy and Climate Research, Forschungszentrum Jülich GmbH, Germany*
[f]*Max-Planck-Institut für Plasmaphysik, Garching, Germany*
[g]*EUROfusion Programme Management Unit, PPPT, Boltzmannstr. 2, D-85748 Garching, Germany*

Abstract

About 85% of the primary energy is currently obtained from fossil sources. In the next future, nuclear fusion can significantly contribute to energy production: the fuel is in principle unlimited and radioactive waste are short lived. Next steps in fusion research are represented by the two tokamaks ITER, which is under construction, and DEMO, which is in its conceptual design phase. In this paper we focus on a specific aspect of DEMO design, that is indeed crucial for tokamak safe operation: plasma vertical and shape control. It is well known that a plasma with elongated cross-section exhibits a vertical instability that needs to be feedback controlled. Typically on operating tokamaks, and in ITER, this task is accomplished using in-vessel actuator coils. Since in the present DEMO design these coils are not foreseen, hereafter we assumed that all the actuator coils, located outside the vessel, are used at the same time to guarantee both vertical stabilization and shape control, resorting to a suitable geometric decoupling. The performance of the controller is shown in simulation using a nonlinear evolution code during a plasma H-L back-transition.

Keywords: Plasma Vertical Stabilization, Magnetic Control, Magnetic Sensors

1. Introduction

This paper describes the preliminary design of a position, current and shape control for DEMO tokamak, based on the availability of magnetic sensors. The controller is designed basing on the CREATE-L model [1] of the DEMO 2017 Single-Null configuration. The design follows the guidelines presented in [2], and it consists of various loops: i) a Vertical Stabilization fast controller; ii) a shape controller; iii) a PF and CS current controller; and iv) the plasma current controller. The controller performance has been assessed in the presence of a given set of events. In this paper we will present the results for a so-called *loss of power* which occurs during a plasma H-L back-transition. In the closed-loop simulations, simplified yet realistic models of the actuators and of the magnetic diagnostics are included.

2. Description of the plant and controller architecture

The interaction between the plasma and conducting structures surrounding can be approximately described around an operational point by the following linearized time-invariant model

$$L_{11}\dot{x}_{PF} + L_{12}\dot{x}_e + E_1\dot{w} = u_{PF} + k_{VS1}u_{VS1} \tag{1a}$$

$$L_{12}\dot{x}_{PF} + L_{22}\dot{x}_e + R_{22}x_e + E_2\dot{w} = 0, \tag{1b}$$

where we use the fact that in DEMO the active coils are superconductive and hence there is no resistive term in the first equation. All the quantities indicate deviations with respect to a nominal value. With the vector x_{PF} we denote the currents in the 11 active coils (6 PF coils and 5 CS coils); with the vector x_e the currents in the passive circuits and the plasma current. The vector w contains the two parameter l_i and β_p, which are assumed to be disturbances, as explained in [1]. Finally the vector u_{PF} contains the voltages provided by the main converters, which have the task to supply the currents needed for scenario and shape control, whereas u_{VS1} is the voltage provided by the fast converter acting on the imbalance circuit (see Fig. 1), whose task is to supply the current needed for vertical stabilization. The imbalance circuit $VS1$ makes use of 4 PF coils; the vector k_{VS1} in (1a) is used to select the coils.

The main converters $VP2 - VP5$ and the imbalance circuit converter $VS1$ act on the same coils $PF2 - PF5$. Hence differently from other tokamaks, where there are coils dedicated to the vertical stabilization of the plasma configuration, in this case it is not possible to have a structural decoupling between the plasma current, position and shape position controller, and the vertical stabilization controller. Since it is convenient to have the possibility to decouple these two controllers, and to design them separately, in this paper we will resort to a geometric decoupling based on a suitable decomposition of the state subspace constituted by the 11 PF and CS coil currents.

As shown in Figure 2, the controller has the following structure:

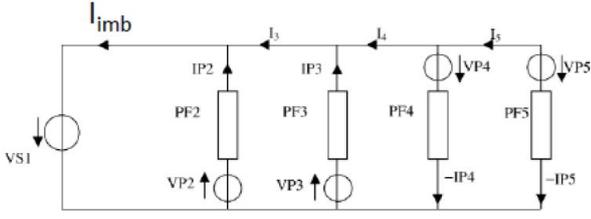*Corresponding author. E-mail: ariola@uniparthenope.it

Figure 1: The imbalance circuit used for DEMO vertical stabilization. This circuit uses 4 PF coils. The imbalance current I_{imb} is given by $I_{imb} = I_{PF2} + I_{PF3} - I_{PF4} - I_{PF5}$.
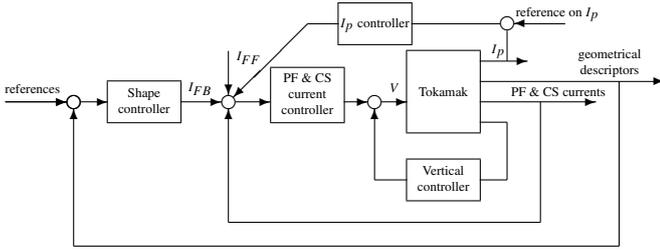

Figure 2: A schematic representation of the plasma control feedback scheme. I_{FF} indicates the scenario feedforward currents, whereas I_{FB} indicates the feedback current deviations; V are the total voltages provided by the main converters.

a) **Plasma current, position and shape controller.** This controller also integrates with the supervisor providing the feedforward (I_{FF}) currents needed to track a desired plasma scenario. This controller is in turn divided in three components: i) Current decoupling controller; ii) Shape controller; iii) Plasma current controller.
b) **Vertical stabilization controller.**

The current decoupling controller acts on an intermediate timescale; its task is to evaluates the voltages to be applied to the plant in order to track the reference PF and CS coil currents which are the sum of the scenario feedforward currents (I_{FF}) and the feedback current deviations (I_{FB}) coming from the shape controller to compensate for unforeseen disturbance. The shape controller acts on a slower timescale with respect to the current decoupling controller. The plasma current controller has the aim of keeping the plasma current close to its reference minimizing the cross-coupling with the shape controller. Finally, the vertical stabilization controller acts on the fastest time scale and uses as actuator the imbalance circuit converter.

3. Controller design

3.1. Design of the current decoupling controller

The design of the current decoupling controller is done on a plasmaless model, by neglecting the presence of the eddy currents in such a way that in dry discharges (i.e. discharges with no plasma) the current references are tracked with a certain accuracy. When the plasma is present, assuming that it has

been vertically stabilized with a suitable separate loop, it acts as a disturbance for this feedback system. Indeed the dynamic evolution of the eddy current is usually much faster than the evolution of the current flowing in the PF and CS coils; hence a singular perturbation approach can be used to reduce the model as it has been shown in [3]. Moreover the presence of the plasma produces only slight modifications to the inductance matrix L_{11}. Under these assumptions, the system equations are then reduced to

$$L_{11}\dot{x}_{PF} = u_{PF} + k_{VS1}u_{VS1}. \qquad (2)$$

The equation of the current decoupling controller are given by

$$u_{PF} = L_{11}\Lambda(x_{PF,ref} - x_{PF}) \qquad (3)$$

where $\Lambda = I/\tau$, being τ an assigned value determining the time constant of a first order circuit which describes the map between the references and the actual values of the PF and CS coil currents. Substituting (3) in (2), the closed loop system equations (again neglecting the eddy currents and the plasma current) are

$$\dot{x}_{PF} = -\Lambda x_{PF} + \Lambda x_{PF,ref} + b_{VS1}u_{VS1}, \qquad (4)$$

where $b_{VS1} = L_{11}^{-1}k_{VS1}$. Recalling that there are 11 active coils, the controllability subspace from the input u_{VS1} is given by

$$X_{VS1} = \mathcal{R}\begin{bmatrix} b_{VS1} & \Lambda b_{VS1} & \cdots & \Lambda^{10}b_{VS1} \end{bmatrix} = \mathcal{R}[b_{VS1}].$$

It follows that the space of the active coil currents is decomposed in two subspaces X_{VS1} and $X_{VS1}^{\perp}$ where $\dim(X_{VS1}) = 1$ and $\dim(X_{VS1}^{\perp}) = 10$. From this, it is clear that the $VS1$ power supply will generate currents which are proportional to the vector b_{VS1}; this fact will be used in the shape controller design.

3.2. Design of the vertical stabilization controller

The vertical stabilization controller is designed on the basis of overall system equation (1) considering the presence of the current decoupling controller (3). Hence the equations read

$$L_{11}\dot{x}_{PF} + L_{12}\dot{x}_e + L_{11}\Lambda x_{PF} + E_1\dot{w}$$
$$= L_{11}\Lambda x_{PF,ref} + k_{VS1}u_{VS1} \qquad (5a)$$
$$L_{12}\dot{x}_{PF} + L_{22}\dot{x}_e + R_{22}x_e + E_2\dot{w} = 0. \qquad (5b)$$

From equation (5a) it is clear that the effect of the current decoupling controller is to introduce a resistance matrix (equal to $L_{11}\Lambda$) in the PF and CS coil circuits. As it is shown for example in [3], when the coils used to vertically stabilize the plasma are superconductive, a constant gain feedback loop on the plasma vertical speed is sufficient to obtain a stable closed loop system; this is no more true when the stabilizing coils are resistive. In these cases the proportional gain on the vertical loop has to be combined with a proportional gain on the currents of the active coil circuits (see for example [4] for the JET tokamak, and [5] for the ITER tokamak).

In DEMO the current generated by the $VS1$ converter is spread (with different weights) to the four coils $PF2 - PF5$,
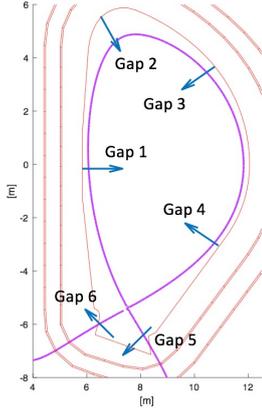
Figure 3: The six gaps that are controlled in DEMO

and, because of the inductive coupling, to all the other coils. Our choice was to feedback together with the vertical speed the projection of the actual PF and CS coil current on the X_{VS1} subspace. Hence the voltage applied to the $VS1$ converter is given by

$$u_{VS1} = k_1 \dot{z} + k_2 T_1^T x_{PF} = k_1 \dot{z} + k_2 x_{VS1}, \qquad (6)$$

where z indicates the plasma centroid vertical position and $T_1 = b_{VS1}/\|b_{VS1}\|$ is an orthonormal basis of X_{VS1}.

3.3. Design of the shape controller

The plasma shape in DEMO is controlled by means of six plasma-wall gaps (see Fig. 3), whose deviations with respect to the nominal values can be described by the linear equation

$$g = C_{g1} x_{PF} + C_{g2} x_e + F_g w. \qquad (7)$$

It can be indeed demonstrated (see [6]) that choosing the gaps in a suitable way, it is possible to control the overall plasma boundary by means only of a "few" gaps. Once the plasma is stabilized by the vertical stabilization controller, on a slow timescale the dynamic system describing the evolution of the gaps can be approximated by

$$\dot{x}_{PF} = -\Lambda x_{PF} + \Lambda x_{PF,ref} \qquad (8a)$$

$$g = C_{g1} x_{PF}. \qquad (8b)$$

The references on the PF and CS coil currents are used to control the selected plasma-wall gaps. Since we want a minimal interaction between the shape and the vertical stabilization controllers, the current references generated by the shape controller should lie on the subspace $X_{VS1}^{\perp}$.

Let T_2 be a matrix whose columns are an orthonormal basis of the $X_{VS1}^{\perp}$ subspace. Recalling that T_1 is a basis of X_{VS1} it holds that $T_2^T T_1 = 0$. Hence we can write

$$x_{PF} = T_1 x_{VS1} + T_2 \tilde{x}_{PF} \qquad (9a)$$

$$x_{PF,ref} = T_2 \tilde{x}_{PF,ref}. \qquad (9b)$$

From (9a) it is straightforward to obtain that

$$\tilde{x}_{PF} = T_2^T x_{PF}.$$

Therefore from (8), recalling that $\Lambda = \frac{1}{\tau} I$, we obtain

$$\dot{\tilde{x}}_{PF} = -\Lambda \tilde{x}_{PF} + \Lambda \tilde{x}_{PF,ref} \qquad (10a)$$

$$g = C_{g1} T_2 \tilde{x}_{PF} + C_{g1} T_1 x_{VS1}. \qquad (10b)$$

The plasma-wall gap controller is chosen to be a multivariable PI controller in the form

$$\tilde{x}_{PF,ref} = K_P(g_{ref} - g) + K_I \mathcal{L}^{-1}\left[\frac{I}{s}\right] * (g_{ref} - g). \qquad (11)$$

The current component x_{VS1} in (10b) is generated by the $VS1$ converter; it acts as a disturbance for the plasma-wall gap controller. Finally the reference to the current decoupling controller is given by (9b)

$$x_{PF,ref} = T_2 \tilde{x}_{PF,ref}.$$

3.4. Design of the plasma current controller

The last loop to be designed is a PI controller on the plasma current. The gains of the PI controllers have been obtained by means of a parametric optimization aimed at minimizing the cross-coupling with the other loops, especially with the shape controller. The settling time has been chosen in the order of 40–50 s.

4. Simulation results

The controller performance has been assessed in the presence of various events; due to the lack of space, hereafter we will only show the case of a so-called *loss of power* which occurs during a plasma H-L back-transition. This disturbance is modeled as a β_p drop of about 0.4 in 4 s while l_i is more or less constant.

The closed-loop simulations have been carried out under the following conditions:

- taking into account voltage saturations on the PF and CS voltages;

- including a simplified, yet realistic model for the actuators, consisting of a first-order filter plus delay in the form $\frac{e^{-s\tau_1}}{1+s\tau_2}$, where the values for the delay τ_1 and the time constant τ_2 have been derived from a study conducted in ITER [7];

- assuming that the various geometric controlled quantities, i.e. the centroid vertical position and the six gaps, are reconstructed basing on the measurements of magnetic sensor located inside the vessel;

- absence of noise on the sensor measurements.

Fig. 4 and Fig. 5 show the results of a linear simulation in presence of the loss of power disturbance, in terms of controlled gap deviations and control power. Under the conditions specified before (use of magnetic in-vessel sensor with no noise), the disturbance is fully controllable, but with a peak active power of about 700 MW. It remains an open issue at this time whether and how the DEMO operator will be able
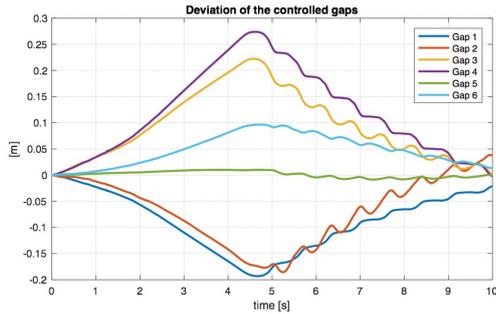
3

Figure 4: Deviation of the controlled gaps during a *loss of power*
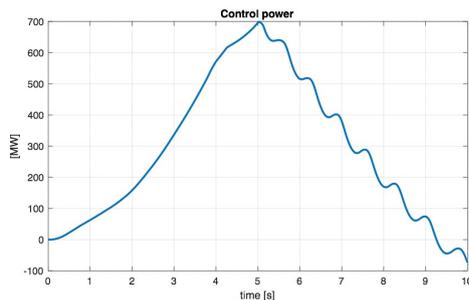

Figure 5: Control power during a *loss of power*

Figure 6: Closed-loop behavior in the presence of a *loss of power* using the CREATE_NL code. The figure shows the plasma boundary before the disturbance is applied (in blue) and the boundary after 4 s, when the plasma–wall distance reaches its minimum of about 6 cm

to provide this amount of control power at any time. Hence the conclusion on the *controllability* of the plasma will depend on the provision of control power. The controller performance have been then tested using the nonlinear evolution CREATE-NL [8] model. The nonlinear simulation confirms the linear prediction: the minimum plasma-first wall distance is of about 24 cm at equilibrium and becomes of about 6 cm after 4 seconds the disturbance is applied, as shown in Fig. 6, where the plasma boundary is shown at $t = 0$ and at $t = 4$ s.

5. Conclusions

In this paper we have presented the preliminary design of a current, position and shape controller for the DEMO tokamak. The controller performance have been tested using the model of the DEMO 2017 Single-Null configuration. At the present stage there are many critical issues that need to be tackled in order to ascertain whether the present DEMO configuration is *controllable* or not:

- in our design we rely on the availability of magnetic sensors located inside the vessel. It is still an open issue whether these sensors can survive the harsh DEMO conditions. The use of alternative sensors, such as microwave reflectometry and other diagnostics like polarimetry/interferometry needs to be investigated;

- the present list of disturbances to be rejected by the controller is still preliminary. Anyway some of the disturbances seem to be hardly controllable: the plasma gets very close to the first wall and/or the needed control
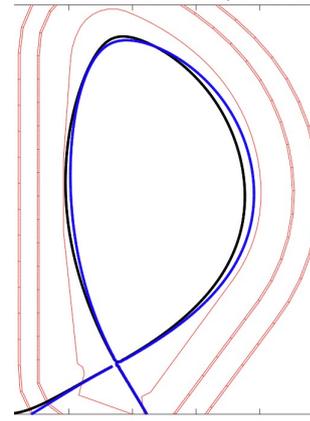
power is very large and the possibility of providing such large amount needs to be ascertained.

The results of the closed-loop simulations are useful to direct the possible modifications of the DEMO design, in order to converge to a DEMO configuration which could guarantee the best possible reliability.

Acknowledgments

References

[1] R. Albanese and F. Villone. The linearized CREATE-L plasma response model for the control of current, position and shape in tokamaks. *Nucl. Fus.*, 38(5):723–738, May 1998.

[2] M. Ariola and A. Pironti. *Magnetic Control of Tokamak Plasmas*. Springer, Second edition, 2016.

[3] M. Ariola and A. Pironti. An Application of the Singular Perturbation Decomposition to Plasma Position and Shape Control. *Eur. J. Control*, 9:410–420, 2003.

[4] M. Lennholm et al. Plasma control at JET. *Fus. Eng. Design*, 48(1–2):37–45, Aug. 2000.

[5] G. Ambrosino, M. Ariola, G. De Tommasi, and A. Pironti. Plasma Vertical Stabilization in the ITER Tokamak via Constrained Static Output Feedback. *IEEE Trans. Contr. Sys. Tech.*, 19(2):376–381, Mar. 2011.

[6] A. Pironti and A. Portone. Optimal choice of the geometrical descriptors for tokamak plasma shape control. *Fus. Eng. Des.*, 43(2):115–127, Dec. 2008.

[7] E. Gaio, R. Piovan, V. Toigo, and I. Benfatto. The control system of the ITER vertical stabilization converter. *Fus. Eng. Des.*, 66–68:719–725, Sept. 2003.

[8] R. Albanese, R. Ambrosino, and M. Mattei. CREATE-NL+: A robust control-oriented free boundary dynamic plasma equilibrium solver. *Fus. Eng. Des.*, 96–97:664–667, Oct. 2015.